

Reduction of $[(C_5Me_5)_2Mo_2O_5]$ and $[(C_5Me_5)_2Mo_2O_4]$ in Methanol/Water/Trifluoroacetate Solutions Investigated by Combined On-Line Electrochemistry/Electrospray-Ionization Mass Spectrometry

Jenny Gun,^[a] Alexandre Modestov,^[a] Ovadia Lev,^[a] and Rinaldo Poli*^[b]

Keywords: Cyclopentadienyl ligands / Electrochemistry / Electrospray-ionization mass spectrometry / Molybdenum / Oxo ligands

Complexes $[Cp^*_2Mo_2O_5]$ ($Cp^* = \eta^5-C_5Me_5$) and $[Cp^*_2Mo_2O_4]$ were investigated by combined on-line electrochemical (EC) reduction and electrospray-ionization mass spectrometry (ESI-MS) techniques in a trifluoroacetic acid buffered water/methanol solution. The reduction products at the larger negative potentials are identical for both compounds. The studies reveal the existence of a wide range of previously unknown di- and trinuclear Mo^V , Mo^{IV} , Mo^{III} , and mixed-val-

ence complexes that were identified on the basis of their masses and characteristic isotope patterns. The structures of the initial compounds and the product of electroreduction with $m/z = 713-729$ were supported by in situ MS^n experiments that allowed the elucidation of the fragmentation pathway for the collision-induced dissociation.

(© Wiley-VCH Verlag GmbH & Co. KGaA, 69451 Weinheim, Germany, 2003)

Introduction

The development of the Electrospray-Ionization Mass Spectrometers (ESI-MS) by Yamashita and Fenn^[1] has provided a very powerful technique for analyzing various charged inorganic,^[2] organic^[3] and organometallic species in solution.^[4] Electrospray ionization at atmospheric pressure is a technique that makes use of an electrostatic sprayer to assist in the transfer of the ionic analytes that are initially present in solution into the gas phase.^[5] In contrast to conventional ionization methods, which create undesirable fragment ions, the ESI technique usually gives simpler spectra.^[6]

The on-line combination of electrochemistry with ESI-MS has been achieved in the last decade. Preparative electrochemistry, followed by ESI-MS analysis of the isolated products or products generated in situ, has been extensively explored by Bond et al.^[7,8] Three other groups, those of Cole et al.,^[9,10] Van Berkel et al.,^[11,12] and Brajter-Toth et al.,^[13] have used an electrochemical cell coupled on-line with mass spectrometry for the investigation of redox reactions.

In our previous publication, which focused only on the reductive process of compound $[Cp^*_2Mo_2O_5]$,^[14] we have shown how, from an analytical point of view, various operating conditions may be optimized to minimize spurious reactions in the electrospray chamber and obtain spectra that reflect compositions in solution. The previous study was carried out in an acetic acid buffered solution and most of the resulting reduction products were found to incorporate the acetate ligand. A subsequent chemical reduction study allowed the isolation and structural characterization of $[Cp^*MoO(O_2CCH_3)]_2$, which is closely related to one of the species observed by EC-ESI-MS.^[15] With the goal of generating more reactive aqua species, and to reach the lower oxidation states of Mo, we have expanded the previous study to solutions containing the stronger trifluoroacetic acid, whose conjugate base has a poorer coordinating ability than does the acetate ion. To verify the electroreduction pathway of the compound $[(C_5Me_5)_2Mo_2O_5]$, we have expanded the electroreduction experiments to the previously described^[16–18] Mo^V compound, $[(C_5Me_5)_2Mo_2O_4]$.

Experiments on sequential product-ion fragmentations (MS^n) by collision-induced dissociation (CID) were performed to elucidate the gas-phase degradation pathway for the starting and product compounds. In general, low-energy CID is a powerful technique because of the simplicity and reliability of performing sequential ion fragmentation MS^n experiments. Collisions between analyte ions and the helium gas, which serves as a damping buffer gas in the ion trap, are used for analyte ion fragmentations and excitations. Collision-induced decomposition produces ionic and neutral species simultaneously in the ion trap. Only the

^[a] Lab Environmental Chemistry, The Casali Institute, The Institute of Chemistry, The Hebrew University of Jerusalem, Jerusalem 91904, Israel
Fax: (internat.) + 972-2/658-6155
E-mail: gunjen@pob.huji.ac.il

^[b] Laboratoire de Synthèse et d'Electrosynthèse Organométalliques, Faculté des Sciences "Gabriel", Université de Bourgogne, 6 Boulevard Gabriel, 21000 Dijon, France
Fax: (internat.) + 33-3/80393720
E-mail: poli@u-bourgogne.fr

charged species, however, can be directly identified using conventional multistage mass spectrometry. The chemical structure of the neutral species can only be hypothesized on the basis of the most-favored fragmentation mechanisms. Valuable information on the molecular structures of organic compounds has also been acquired by ESI-MSⁿ, but very few investigations have been conducted with organometallic compounds.^[19,20]

Results and Discussion

Positive-Mode ESI-MS Spectra of the Starting Compounds

The positive-mode ESI-MS spectra of the starting compounds are shown in Figure 1, frames A and B. The inserts show the characteristic isotopic patterns of mono-, di-, and trinuclear Mo fragments. For mononuclear Mo species, the isotopic envelope consists of seven lines with two gaps located between the first and second and the sixth and seventh lines, respectively. The isotopic envelope of a dinuclear Mo ion consists of 14 peaks and has a width of 16 m/z units, while that of a trinuclear Mo species has a width of 23 m/z units. The width of the isotopic envelope is an important characteristic in our MSⁿ fragmentation experiments for the perfect isolation of the whole set of the molecules with the same structure. We shall refer to the various species by the value of m/z of the full isotopic pattern in the isotopic distribution and compare it to the calculated distributions^[21] for the molecular assignment.

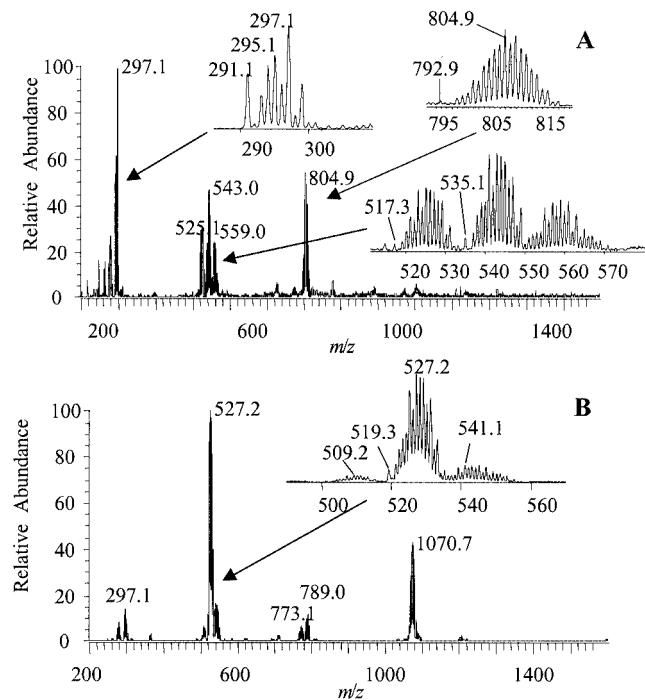


Figure 1. Positive-mode electrospray mass spectra in a mixture of 0.1 M CF_3COOH in $H_2O/MeOH$ (1:1) (pH = 1.2) of (A) $[Cp^*_2Mo_2O_5]$ (0.1 mM) and (B) $[Cp^*_2Mo_2O_4]$ (0.1 mM)

Spectrum A was measured from a water/methanol solution of $[Cp^*_2Mo_2O_5]$ containing 0.1 M trifluoroacetic acid.

It reveals three major regions of peaks, corresponding to mono-, di-, and trinuclear species, respectively. The ESI-MS spectrum of this compound in water/methanol containing 0.1 M ammonium acetate (pH = 4) has been described previously.^[14] The lower pH (pH = 1.8) used in the present study changes the product distribution significantly in every region. The mononuclear region exhibits the $[Cp^*MoO_2]^+$ peak ($m/z = 259-267$) and the $[Cp^*MoO_3H_2]^+$ peak ($m/z = 277-285$) at approximately the same relative intensity as in the previous acetate buffer study. The strongest peak, however, corresponds to the methanol addition product, $[Cp^*MoO_2(MeOH)]^+$ ($m/z = 291-299$), which has only a very small intensity in the acetic buffer. The formation of adducts with solvent molecules in the ion trap is a well-known phenomenon.^[22,23]

The main peak for dinuclear species corresponds to the protonated starting compound $[Cp^*_2Mo_2O_5H]^+$ ($m/z = 535-551$), as it was in the corresponding study in the acetic acid buffer.^[14] The other most pronounced dinuclear peaks, corresponding to daughter ions formed in the ESI-MS chamber, had not been described previously, since their intensity was much lower when measured from the higher pH conditions. These dinuclear peaks increase in relative abundance with increasing temperatures of the heated capillary. The lighter set of peaks ($m/z = 517-533$) corresponds to the loss of one water molecule. This process must, of course, involve at least one of the Cp^* methyl group's H atoms, leading to a tetramethylfulvene ligand. Therefore, the peak is assigned to complex $[Cp^*(C_4Me_4CH_2)Mo_2O_4]^+$. The methylene group of this ligand may be bonded to the molybdenum atom or to one of the oxygen atoms. The envelope at higher masses, on the other hand, results from the superposition of two envelopes, one (major) at $m/z = 549-565$ that is attributed to a MeOH adduct of the tetramethylfulvene complex just described, and one (minor) at $m/z = 553-569$ that probably results from the addition of water to the starting compound. The $[Cp^*_3Mo_3O_7]^+$ peak ($m/z = 793-816$) is the only relevant feature in the region of the trinuclear species.

The differences between Figure 1 and the corresponding spectrum from the experiment with the acetic acid buffer (see Figure 1 of ref.^[14]) are consistent with our parallel speciation studies. We have shown that the complex $Cp^*MoO_2^+$ is the predominant species at pH < ca. 3, while a mixture of $[Cp^*MoO_2]^+$ and $[Cp^*MoO_3]^-$ {in equilibrium with $[Cp^*MoO_2(OH)]$ and $[Cp^*_2Mo_2O_5]$, depending on the $H_2O/MeOH$ ratio} is present at a pH of ca. 4.^[24] Indeed, the peaks corresponding to the dinuclear $[Cp^*_2Mo_2O_5]$ species are less abundant at the lower value of pH, while all those related to species $[Cp^*MoO_2]^+$ (mononuclear and trinuclear species) are comparatively more abundant. Indeed, the trinuclear species results from the addition of $[Cp^*MoO_2]^+$ to $[Cp^*_2Mo_2O_5]$ (vide infra).

The ESI-MS investigation of complex $[Cp^*_2Mo_2O_4]$, reported here for the first time, was carried out under the same conditions used for compound $[Cp^*_2Mo_2O_5]$, to allow comparisons to be made. The spectrum of the starting solution is shown in Frame B of Figure 1. The main peak corre-

sponds to the protonated starting compound, $[(C_5Me_5)_2Mo_2O_4H]^+$ ($m/z = 519-535$), and the second-most important component ($m/z = 1058-1085$) is assigned to the tetranuclear $[Cp^*_4Mo_4O_6(OH)_3]^+$ complex. The latter is formally obtained by dimerization of the starting compound and addition of a water molecule and a proton. Evidence for the existence of a tetranuclear species has been provided for the corresponding Cp system.^[25] The spectrum shows fewer peaks relative to that of the pentaoxo analogue. This situation can result from either a simpler composition in solution (the speciation of this compound in methanol/water is yet unknown) or from a greater gas-phase stability and, therefore, a less pronounced collision-induced decomposition. Both compounds adopt a neutral molecular structure in organic solvents.^[16,26] To further explore this point, we proceeded with a detailed investigation of the gas-phase stability and MS^n fragmentation pathways of the starting compounds.

Gas-Phase Stability of the Starting Compounds

Figure 2 shows the relative abundances of the peaks of the starting compound ($m/z = 535-551$ for $[Cp^*_2Mo_2O_5H]^+$ and $m/z = 519-535$ for $[Cp^*_2Mo_2O_4H]^+$) as a function of the applied collision energy during the collision-activated decomposition events in the ion-trap mass spectrometer. Both dissociation profiles lead to S-shaped curves. The half-wave collision energy ($E_{1/2}$) corresponds to the energy (in the percentage of the maximum tickling voltage) at which the relative abundance as a fraction of the total ion current of the starting ion is 0.5.^[27-30] For the same charge state (+1), the larger the value of $E_{1/2}$ the more stable is the compound in the gas phase. As it is evident from Figure 2, the value of $E_{1/2}$ of $[Cp^*_2Mo_2O_4]$ is almost twice that of $[Cp^*_2Mo_2O_5]$, which underscores the greater gas-phase stability of the former compound. This difference can be rationalized rather easily on the basis of the known structural and bonding differences between the two compounds. While the tetraoxo Mo^V complex contains a direct metal-metal bond and two oxo bridges, the pentaoxo compound contains one oxo bridge and no metal-metal interactions.

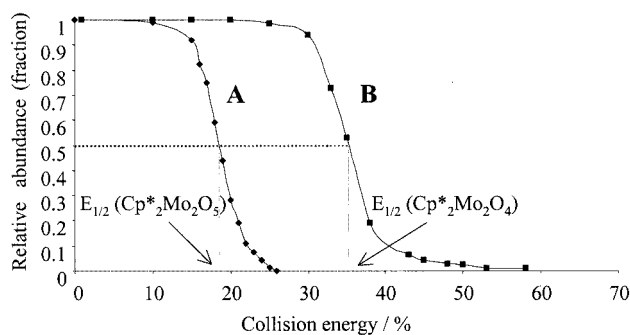


Figure 2. Dissociation profiles of the starting compounds {(A) $[Cp^*_2Mo_2O_5]$ and (B) $[Cp^*_2Mo_2O_4]$ } in the same charge state as a function of increased collision energy in the ion trap; the solutions are as described in Figure 1

Fragmentation Pathways of the Starting Compounds

The dissociation profiles provided us with information about the stability of $[Cp^*_2Mo_2O_5]$ and $[Cp^*_2Mo_2O_4]$ complexes in the ion trap. An analysis of their degradation in the ion trap was carried out by their isolation therein, followed by the observation of their sequential multistep dissociations (MS^n experiments). The main results for $[Cp^*_2Mo_2O_5]$ and $[Cp^*_2Mo_2O_4]$ are shown in frames A and B of Figure 3, with the proposed fragmentation pathways in Schemes 1 and 2, respectively.

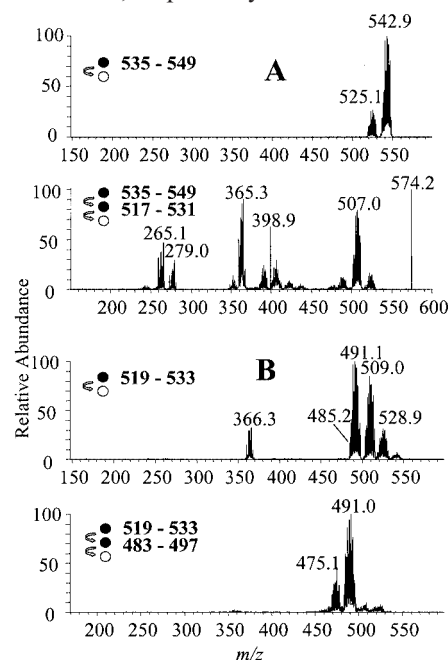
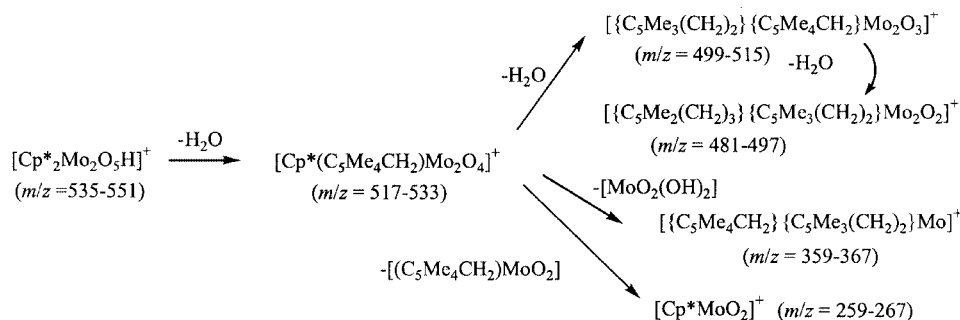


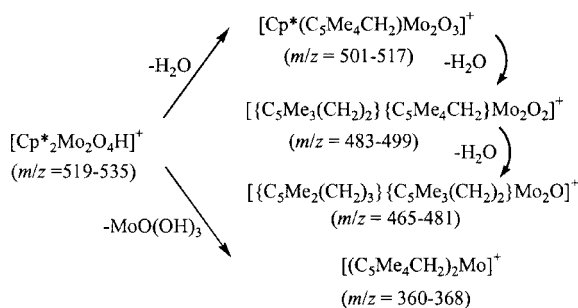
Figure 3. MS^n fragmentation pathways of compounds $[Cp^*_2Mo_2O_5]$ (A) and $[Cp^*_2Mo_2O_4]$ (B); the solutions are the same as those described in Figure 1

As concluded above from the dissociation profiles, $[Cp^*_2Mo_2O_5]$ is less stable than $[Cp^*_2Mo_2O_4]$ in the ion trap. The spectrum in Figure 3 (A) shows that the first CID step for the $[Cp^*_2Mo_2O_5H]^+$ ion generates only one daughter ion ($m/z = 517-533$) by loss of a water molecule. MS^3 fragmentation of this daughter ion leads to many products by further loss of water and of a neutral (fulvene)-dioxomolybdenum fragment. To the best of our knowledge, the C-H activation of a Cp^* methyl group, that is associated to the elimination of a water molecule and to the transformation to a tetramethylfulvene ligand, has not been highlighted previously in an MS study. There is, however, at least one precedent in solution chemistry for compound $[Cp^*RuCl_2]_2O$.^[31]

The main peaks are tentatively assigned in Scheme 1, although it is not possible to establish the particular methyl group that furnishes the hydrogen atoms. The $m/z = 359-367$ peak has the characteristic shape of a monomolybdenum species and is not observed at all in the regular ESI-MS. This compound would result from the elimination of a molybdic acid molecule with the abstraction of two H atoms from the Cp^* methyl groups. This assignment is in



Scheme 1



Scheme 2

further agreement with related fragmentations of more reduced species, as will be shown later. We point out further that the exact structure of the proposed species containing two or more activated Me groups, e.g., $[(\text{C}_5\text{Me}_4\text{CH}_2)_2\text{Mo}]^+$ or $[\{\text{C}_5\text{Me}_2(\text{CH}_2)\}\{\text{C}_5\text{Me}_3(\text{CH}_2)_2\}\text{Mo}_2\text{O}]^+$, may implicate the formation of C–C or C–O bonds.

The CID of complex $[(C_5Me_5)_2Mo_2O_4]$ gives fewer peaks than its pentaoxo analogue. Most dinuclear peaks are related for the two compounds (16 fewer mass units corresponding to one oxygen atom). The main mononuclear peak ($m/z = 360-369$) is one mass unit higher than the main mononuclear peak derived from the pentaoxo solution, and, thus, the peak indicates that it is a one-electron-reduced form of it. The peak probably derives from the expulsion of a $MoO(OH)_3$ species from the parent dinuclear Mo^V complex, paralleling exactly the formation of the mononuclear species in Scheme 1.

Electrochemical Experiments

Figure 4 shows the voltammogram recorded in our flow-through electrochemical cell in parallel with the ESI-MS measurements. Curve A shows the background voltammogram, whereas curves B and C show the voltammograms of the $[\text{Cp}^*_2\text{Mo}_2\text{O}_4]$ and $[\text{Cp}^*_2\text{Mo}_2\text{O}_5]$ solutions, respectively. As the Mo concentration is identical for both solutions, any difference between curves B and C must be attributed to the difference in the oxidation state of the Mo atom in the starting compound. This assumption is supported by the volt-spectrogram of $[\text{Cp}^*_2\text{Mo}_2\text{O}_5]$ (vide infra), which clearly

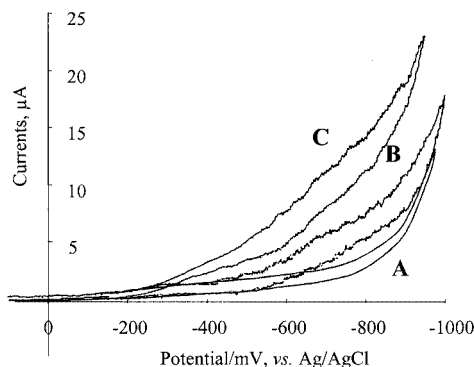


Figure 4. Cyclic voltammograms taken during the on-line combined EC/ESI-MS experiments. (a) blank solution; (b) 1.1 mM $[\text{Cp}^*\text{2Mo}_2\text{O}_4]$; (c) 1.1 mM $[\text{Cp}^*\text{2Mo}_2\text{O}_5]$, in $\text{H}_2\text{O}/\text{MeOH}$ (1:1) containing CF_3COOH (0.1 M; $\text{pH} = 1.2$); scan rate: 0.5 mV/s

indicates that the electroreduction of $[\text{Cp}^*_2\text{Mo}_2\text{O}_5]$ proceeds through the formation of $[\text{Cp}^*_2\text{Mo}_2\text{O}_4]$.

The current–potential curves at the forward and backward scans are in parallel for both compounds and the heights are virtually independent of the scan rate over a rather wide range of scan rates (up to $100 \text{ mV}\cdot\text{s}^{-1}$). This observation means that the electrochemical reduction of both $[\text{Cp}^*_2\text{Mo}_2\text{O}_4]$ and $[\text{Cp}^*_2\text{Mo}_2\text{O}_5]$ is apparently controlled by an interfacial step rather than being limited by diffusion. In separate studies that are out of the scope of this paper, we have witnessed the formation of a polymer film on the electrode surface under the conditions of electroreduction. This phenomenon makes it impossible, solely on the basis of the voltammetric experiments, to elucidate the mechanisms of electroreduction of $[\text{Cp}^*_2\text{Mo}_2\text{O}_4]$ and $[\text{Cp}^*_2\text{Mo}_2\text{O}_5]$ and identify the electroreduction products.

Coupled Electrochemistry/ESI-MS Studies: Consumption of the Starting Species

The coupled EC/ESI-MS study was carried out with a slow (0.5 mV/s) linear potential sweep between 0 and -1 V, and then back again to 0 V, similar to the experiment described in our previous study.^[14] Figure 5 shows the volt-spectrograms of the major mono-, di-, and trinuclear species. During the backward, anodic scan, the concentration profiles follow approximately the same pattern observed in

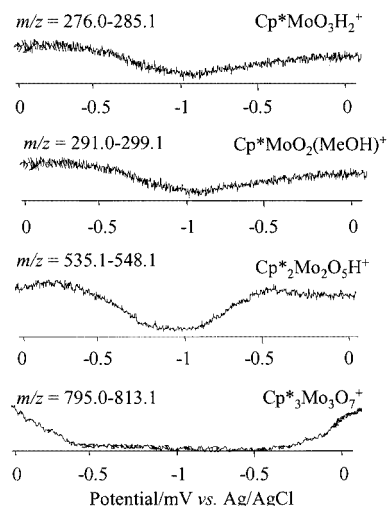


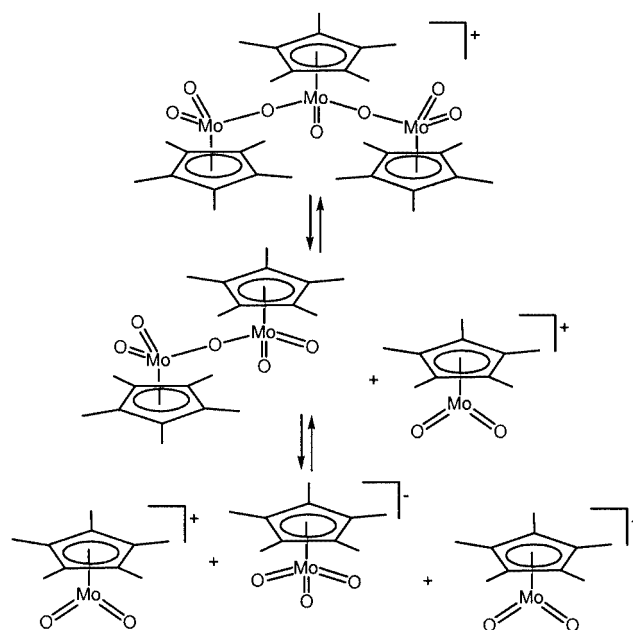
Figure 5. Dependence on potential of the relative abundance of the starting species during the coupled electrochemistry/ESI-MS of $[\text{Cp}^*_2\text{Mo}_2\text{O}_5]$; the experimental conditions are the same as those described in Figure 4

the cathodic scan, indicating that the experiment is not polluted by film deposition processes.

The concentrations of both mononuclear species and of the dinuclear species start to decrease at a potential slightly less negative than $E = -0.5$ V. The trinuclear species, on the other hand, decreases in concentration much earlier, at $E \approx 0$ V, and reaches a minimum at $E = -0.5$ V. This result shows unambiguously that the trinuclear species must be present already in solution. If it had formed by a combination of $[\text{Cp}^*\text{MoO}_2]^+$ and $[\text{Cp}^*_2\text{Mo}_2\text{O}_5]$ in the spectrometer chamber only, its abundance would not decrease prior to that of either of the two other species. The reduction of the trinuclear species is thermodynamically easier than those of the mono- and dinuclear species, probably because of the metal–metal bond formation that is expected to accompany the process (vide infra). Since we have shown that a water-rich environment favors the spontaneous ionization of $[\text{Cp}^*_2\text{Mo}_2\text{O}_5]$ into $[\text{Cp}^*\text{MoO}_2]^+$ and $[\text{Cp}^*\text{MoO}_3]^-$, we propose equally that the trinuclear species is derived from the combination of $[\text{Cp}^*\text{MoO}_3]^-$ with two $[\text{Cp}^*\text{MoO}_2]^+$ ions, as shown in Scheme 3.

Electrochemical Formation of Reduced Dimer Compounds

Figure 6 shows the mass spectrum of the $[\text{Cp}^*_2\text{Mo}_2\text{O}_5]$ solution recorded at -1 V. Several new peaks, assigned to electroreduction products, are evident in this spectrum. Some of these peaks are associated with reduction products that are identical with, or related to, those observed previously under the same conditions in an acetic acid buffer (i.e., $[\text{Cp}^*_2\text{Mo}_2\text{O}_4\text{H}]^+$, $m/z = 519-535$). Other peaks, on the other hand, correspond to new species {i.e., $[\text{Cp}^*_2\text{Mo}_2(\text{OH})(\text{O}_2\text{CCF}_3)_2]^+$, $m/z = 697-715$; $[\text{Cp}^*_2\text{Mo}_2\text{O}(\text{OH})(\text{O}_2\text{CF}_3)_2]^+$, $m/z = 713-729$; $[\text{Cp}^*_2\text{Mo}_2\text{O}_3(\text{O}_2\text{CCF}_3)]^+$, $m/z = 615-633$ }. The nature and the intensity/potential profiles of all electroreduction products obtained from the $[\text{Cp}^*_2\text{Mo}_2\text{O}_4]$ solution are identical with those derived from



Scheme 8

the pentaoxo solution. This observation indicates that all reduced products obtained from the pentaoxo solution are formed through the intermediacy of the tetraoxo complex.

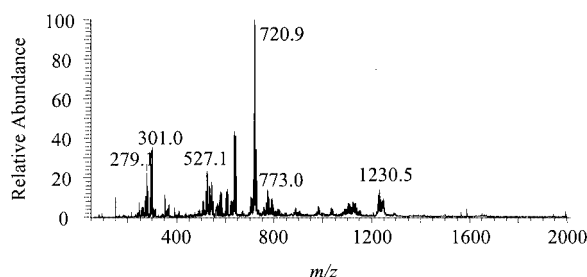


Figure 6. Positive-mode electrospray mass spectra in 0.28 mM CF_3COOH , $\text{H}_2\text{O}/\text{MeOH}$ (1:1) (pH = 1.2) of $[\text{Cp}^*_2\text{Mo}_2\text{O}_5]$ (1.1 mM) after reduction ($E = -1$ V)

Figure 7 depicts volt-spectrograms of a few selected reduced dinuclear products, namely two $\text{Mo}^{\text{V},\text{V}_2}$ species, $[\text{Cp}^*_2\text{Mo}_2\text{O}_4\text{H}]^+$ and $[\text{Cp}^*_2\text{Mo}_2\text{O}_3(\text{O}_2\text{CCF}_3)]^+$, a $\text{Mo}^{\text{IV},\text{IV}}$ species, $[\text{Cp}^*_2\text{Mo}_2\text{O}(\text{OH})(\text{O}_2\text{CCF}_3)_2]^+$, and a $\text{Mo}_2^{\text{III},\text{III}}$ species, $[\text{Cp}^*_2\text{Mo}_2(\text{OH})(\text{O}_2\text{CCF}_3)_2]^+$, together with their corresponding MS isotopic pattern and a tentatively assigned structure. Interestingly, the major electroreduction products observed in the current study are derived from subsequent two-electron addition processes, whereas the previous study in the acetic acid buffer also showed a dinuclear mixed-valence ($\text{Mo}^{\text{IV},\text{V}_2}$) species. Mononuclear (acetato) Mo^{V} and $-\text{Mo}^{\text{IV}}$ complexes were also evident in the previous study, but the corresponding trifluoroacetato species are not observed in the present investigation.

Another notable difference is that, whereas the observed $\text{Mo}^{\text{V},\text{V}_2}$ products have the same stoichiometry under both

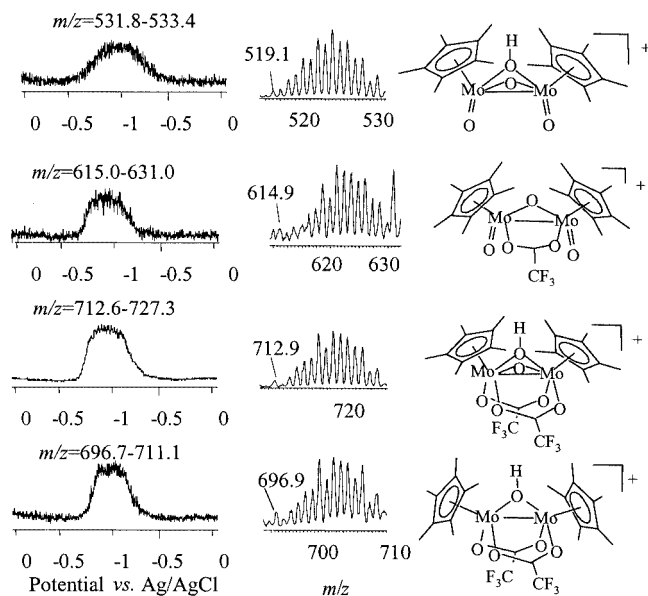
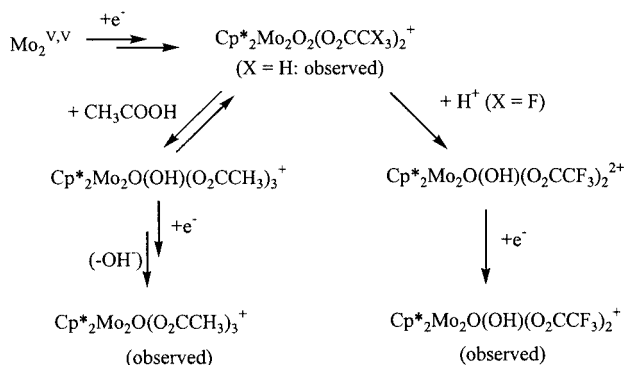


Figure 7. Dependence on potential of the relative abundance of the dinuclear species generated during the coupled electrochemistry/ESI-MS of $[Cp^*_2Mo_2O_5]$; left: volt-spectrograms with the range of m/z used for the integration; center: expanded isotopic pattern; right: tentative chemical structure; the experimental conditions are identical to those of Figure 5

conditions, the $Mo^{IV,IV}_2$ product is $[Cp^*_2Mo_2O(OH)(O_2CCF_3)_2]^+$ in the present study and $[Cp^*_2Mo_2O(O_2CCH_3)_3]^+$ in the previous acetate study. A peak for the corresponding $[Cp^*_2Mo_2O(O_2CCF_3)_3]^+$ ion is not observed in the present study. This result seems counterintuitive, because the stronger trifluoroacetic acid should be better suited to replace the hydroxo ligand. A possible, though somewhat speculative, interpretation relies on two fundamental differences between the two acids and the corresponding conjugate bases: while CF_3COOH is the stronger acid, CH_3COO^- is the better coordinating agent. Thus, reduction of the same $[Cp^*_2Mo_2O_3(O_2CCX_3)]^+$ ($Mo^{V,V}_2$; $X = H, F$) complex would lead to the same $[Cp^*_2Mo_2O_2(O_2CCX_3)_2]^+$ ($Mo^{IV,V}_2$) ion according to Scheme 4. This ion, however, would be observed only for the acetate system, because with the stronger acid (CF_3COOH) it would immediately be protonated. The CH_3COOH system could, on the other hand, lead to a triacetato species because of the stronger coordinating properties of the acetate ion. If this hypothesis holds true, each final $Mo^{IV,IV}_2$ product would be observed merely because the exchange process between hydroxide and (trifluoro)acetate, though thermodynamically favorable, is too slow under the present conditions. It is also worth mentioning that the neutral diacetato compound $[Cp^*_2Mo_2O_2(O_2CCH_3)_2]$ (i.e., a deprotonated version of the observed product for the trifluoroacetato system) has been isolated from a reductive chemical synthesis and characterized crystallographically.^[15]

While electroreduction did not afford any dinuclear ions with oxidation states below IV when carried out in an acetic acid buffer, it also provides a $Mo^{III,III}_2$ complex in the pres-



Scheme 4

ence of trifluoroacetic acid. This difference may again be attributed to the stronger acidity of CF_3COOH , which favors protonation of the oxo ligands and their elimination as water molecules.

The following approximate potential values for the appearance of every reduced dinuclear species may be measured on the volt-spectrograms in Figure 7: $[Cp^*_2Mo_2O_4H]^+$ ($Mo^{V,V}_2$), -0.55 V; $[Cp^*_2Mo_2O_3(O_2CCF_3)]^+$ ($Mo^{V,V}_2$), -0.60 V; $[Cp^*_2Mo_2O(OH)(O_2CCF_3)_2]^+$ ($Mo^{IV,IV}_2$), -0.68 V; $[Cp^*_2Mo_2O(O_2CCF_3)_2]^+$ ($Mo^{III,III}_2$), -0.76 V. A comparison of the onset reduction potentials with those observed in the previous acetate study is useful. The $[Cp^*_2Mo_2O_4H]^+$ product is not acid dependent. In both studies, the onset of this peak is at approximately the same potential as the onset for the $[Cp^*_2Mo_2O_5H]^+$ consumption and the two numerical values are quite similar (these numbers may be measured only with limited precision). The $[Cp^*_2Mo_2O_3(O_2CCF_3)]^+$ $Mo^{V,V}_2$ species starts to form at a more negative potential relative to the acetato analogue (-0.55 V). Further reduction to the $Mo^{IV,IV}_2$ species seems easier for the trifluoroacetato system, which is in agreement with expectations [cf. reduction at -0.74 and -0.78 V for the (acetato) $Mo^{IV,V}_2$ and $-Mo^{IV,IV}_2$ products, respectively]. Furthermore, reduction to the $Mo^{III,III}_2$ product starts at an even lower potential, while this process is not observed for the acetato system, as mentioned above.

Structural Elucidation of the Product at $m/z = 713-729$

The main product of the electroreductions of both $[Cp^*_2Mo_2O_5]$ and $[Cp^*_2Mo_2O_4]$, namely the $Mo^{IV,IV}_2$ ion interpreted as $[Cp^*_2Mo_2O(OH)(O_2CCF_3)_2]^+$, was the subject of more detailed MSⁿ studies. There are two reasons for choosing to study this product. First, we wanted to prove the general approach of our product identification. Second, we wanted to check whether any observed peaks are, in fact, attributable to daughter ions of this major peak, rather than to primary products of the electrochemical reduction.

Figure 8 shows the main results of the MSⁿ experiment. The spectrum shown in part A is produced from the isolation of the species at $m/z = 713-729$ and subsequent CID. There are four main daughter-ion products, the main

one being that with $m/z = 599-615$. In fact, the lighter products increase in subsequent MS^n experiments, while the heavier one (32 mass units higher) is obviously the solvent (methanol) adduct formed by gas-phase reactions in the ion trap.^[28] This assignment is further supported by the next MS^n step. The product ion at $m/z = 599-615$ was isolated and subjected consequently to further collision activation (MS^3), giving the spectrum shown in Figure 8 (B). The further generation of the peak at $m/z = 634-650$ can be understood easily in terms of the formation of the solvent adduct. Additional fragmentation by CID (MS^4) of the product ion with $m/z = 502-518$ results in one main product with $m/z = 485-501$ and a mononuclear peak with $m/z = 361-369$ [see Figure 8 (C)].

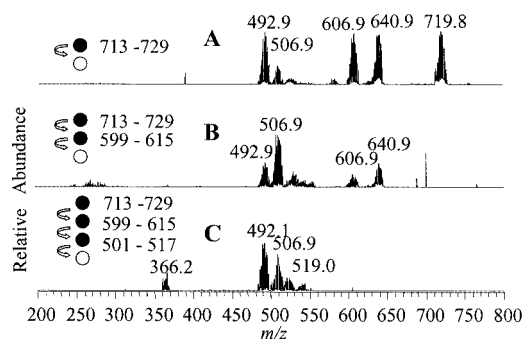


Figure 8. Structural elucidation by MS^n of the main product ($m/z = 713-729$) of the reduction of $[Cp^*_2Mo_2O_5]$ and $[Cp^*_2Mo_2O_4]$

The proposed product ion compositions and fragmentation pathways are shown in Scheme 5. The first fragment ($m/z = 599-615$) results from the loss of 114 units, which corresponds to the molecular weight of trifluoroacetic acid. Therefore, this fragment is still a dinuclear compound of Mo^{IV} . Under the conditions of the experiment (CID = 30% for every MS^n step), the next step of the fragmentation results in a prominent peak with the loss of 97 units, corresponding to a trifluoroacetyl group, and a minor peak with the loss of an additional 17 units (OH). The latter peak becomes the prominent one in the MS^4 . Loss of the acetyl group results in a formal oxidation to a mixed-valence $Mo^{IV,V}_2$ ion that is not observed under the electroreduction conditions, whereas the subsequent loss of OH reforms a $Mo^{IV,V}_2$ ion. The OH and $MoO_2(OH)$ expulsion processes must involve one of the Cp^* methyl group protons to yield a tetramethylfulvene ligand, as already observed above for the CID of the starting complexes. It is quite interesting to observe that, for the three fragmentation processes leading from dinuclear to mononuclear species with loss of a neutral inorganic Mo complex, the latter always corresponds to an oxide/hydroxide in the highest possible oxidation state; i.e., Mo^{VI} from $Mo^{VI,V}_2$ (Scheme 1), Mo^V from $Mo^{V,V}_2$ (Scheme 2), and Mo^V from $Mo^{IV,V}_2$ (Scheme 5).

We conclude from Scheme 5 that the fragmentation pathway undertaken by the compound at $m/z = 713-729$ is similar to that of the starting compounds. It is noteworthy

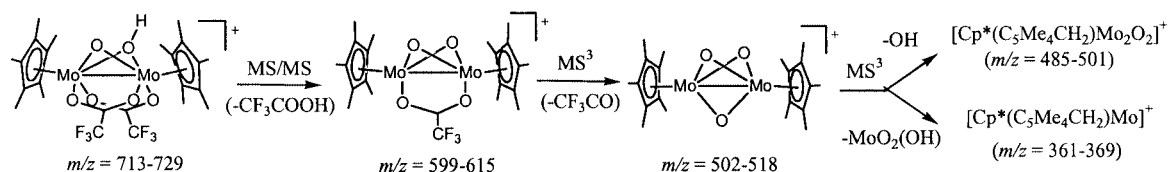
that the peaks at $m/z = 485$ and 361 , generated by MS^4 , are related to the fragments obtained from the Mo^{VI} precursor [$m/z = 481$ and 359 , see Figure 3 (A)] and to those obtained from the Mo^V precursor [$m/z = 483$ and 360 , see Figure 3 (B)]. Therefore, these mass values further support the notion that the ion at $m/z = 713-729$ corresponds to a $Mo^{IV,V}_2$ complex.

Electrochemical Formation of Reduced Trinuclear Species

As can be seen by comparing Figures 1 and 6 there are prominent spectral changes in the trinuclear m/z region following the electrochemical reduction. Volt-spectrograms of the reduced trinuclear compounds are presented in Figure 9. Because of overlap between the isotopic envelopes of different trinuclear species, the volt-spectrogram integrations were carried out over limited ranges of m/z rather than over the entire envelope. The ranges used for the integrations are marked in the figure. As for the previous study with the acetic acid buffer, the envelope of the reduced trinuclear species is shifted by exactly 16 units to a lower value of m/z relative to its precursor complex $[Cp^*_3Mo_3O_7]^+$, suggesting its formulation is that of a proton-free hexa-oxo species. In contrast to the previous study with the acetic acid buffer, on the other hand, further reduction occurs with successive steps of oxygen atom removal, resulting in the observation of $[Cp^*_3Mo_3O_6]^+$ ($Mo^{V,V,V}_3$), $[Cp^*_3Mo_3O_5]^+$ ($Mo^{IV,V,V}_3$), and $[Cp^*_3Mo_3O_4]^+$ ($Mo^{IV,IV,IV}_3$). Once again, this behavior can be attributed to the stronger acidity of CF_3COOH . As for the dinuclear products discussed above, the formation of the trinuclear species in trifluoroacetic acid takes place through two-electron-transfer steps and the reduction potential becomes more negative as the oxidation state decreases. The onset potential values for the various reduced species, as measured from the volt-spectrograms in Figure 9 are, in order of decreasing number of oxygen atoms, -0.54 , -0.61 , and -0.75 V, respectively.

The structures assigned to various reduced species are only tentative and are drawn on the basis of the maximum symmetry principle. A $[(Cp^*Mo)_3(\mu-O)_6]$ core has been shown to exist in complex $[(Cp^*Mo)_3(\mu_2-OH)_n(\mu_2-O)_{6-n}]^{2+}$ (the value of n , probably 5, was not clearly established in the X-ray study)^[32] and in related $[Cp^*_4Mo_5O_{11}]$ and $[Cp^*_6Mo_8O_{16}]$ clusters.^[32,33] The oxidation state in these Mo_3O_6 cores, however, is lower ($Mo_3^{11+} - Mo_3^{14+}$). The dicationic $Mo_3(\mu_3-O)_2(\mu_2-O)_3$ unit is quite common in inorganic clusters, but has not been found as yet, to the best of our knowledge, for Cp^* -substituted triangular clusters of any metal. Finally, the monocapped $Mo(\mu_3-O)(\mu_2-O)_3$ unit is also common for inorganic clusters. The first documented example containing half-sandwiched metal atoms comes from our own recent study of the chemical reduction of $[Cp^*_2Mo_2O_5]$ by zinc in methanol/water containing CF_3COOH .^[34] The isolated compound contains the $[(Cp^*Mo)_3(\mu_3-O)(\mu_2-O)_3(\mu_2-O_2CCF_3)_3]^+$ ion, corresponding to a $Mo^{V,V,V}_3$ species.

No trinuclear species containing trifluoroacetate groups was detected in the present study, suggesting that this weakly coordinating anion has a high tendency to remain



Scheme 5

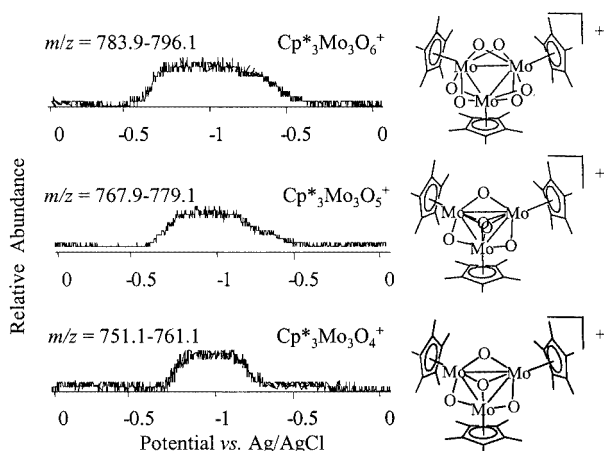


Figure 9. Volt-spectrograms of trimeric species generated during the coupled electrochemistry/ESI-MS of $[Cp^*_2Mo_2O_5]$, including the range of m/z used for the integration and the chemical formula; the experimental conditions are the same as those in Figure 4

dissociated in the highly dielectric aqueous medium. The isolation of the $[(Cp^*Mo)_3O_4(O_2CCF_3)_3]^+$ ion mentioned above, on the other hand, suggests the existence of a transient $[(Cp^*Mo)_3O_4]^{4+}$ species. Therefore, it is quite likely that a much wider variety of $[(Cp^*Mo)_3O_n]^{m+}$ derivatives may be isolated under different conditions of pH, solvent, and counterion. It is also likely that these complexes display very rich redox chemistry. Further synthetic studies are currently ongoing to test these hypotheses and to test the electrofunctionalization of organic substrates for possible catalytic applications.

Conclusion

The present study has provided new information on the nature of the $[Cp^*_2Mo_2O_5]$ in an aqueous medium and on electrochemical versatility of Cp^*Mo species in water. Selected molecular structure assignments from values of m/z and isotopic distributions for Cp^*Mo^V and Cp^*Mo^{IV} reduction products were confirmed by MS^n fragmentation experiments in comparison with those of the Cp^*Mo^{VI} precursor. The study has shown that the lower pH conditions established by CF_3COOH provide access to a Cp^*Mo^{III} species, while reduction under acetic acid conditions went down as far as the oxidation state IV. The study has confirmed the robustness of the Cp^*-Mo bond under aqueous conditions. Even at very low pH, there is no sign of the forma-

tion of species deriving from protonolysis of this bond. This feature, together with the proven rich redox chemistry of the system, holds promise for potential electrocatalytic applications in an aqueous environment.

Experimental Section

General Remarks: The starting compounds, $[(C_5Me_5)_2Mo_2O_5]$ and $[(C_5Me_5)_2Mo_2O_4]$, were prepared according to the literature procedure.^[18] Unless otherwise stated, all solutions of test compounds were prepared in $H_2O/MeOH$ mixture (1:1 by volume) containing 0.1 M CF_3COOH . CF_3COOH was purchased from Aldrich. HPLC-grade methanol was purchased from Baker. The water was triply distilled.

Electrospray Mass Spectrometry with an Ion Trap: A Finnigan (San Jose, USA) LCQ quadrupole ion-trap mass spectrometer equipped with an electrospray-ionization (ESI) interface was used for data acquisition. The ESI was operated in the positive-ion mode with a spray voltage of 4.5 kV, a capillary voltage of 3.5 V, and a source temperature of 120 °C. Mass spectra were obtained by scanning the mass analyzer from $m/z = 100-2000$ with a total of 5 microscans. The maximum injection time into the ion trap was 50 ms. The analyzer was operated at a background pressure of $2 \cdot 10^{-5}$ Torr. In all experiments, helium was introduced at an estimated pressure of 1 mTorr to improve the ion-trapping efficiency. The background helium also served as a collision gas during collision-activated decomposition events. The compounds were isolated in the ion trap with isolation width of 15 m/z units and were activated by using increased collision energy to obtain collision-energy-dissociation profiles.

Coupled Electrochemistry/Electrospray Mass Spectrometry: The electrochemical part of the experimental setup consisted of a PARC 273 potentiostat/galvanostat (Princeton, USA), connected to a specially designed flow-through electrochemical cell that has been described and characterized elsewhere.^[35] The schematic of the electrochemical flow cell is shown in Figure 10. The working glassy-carbon-disk electrode (1) (Metrohm, Herisau, Switzerland), is placed on the bottom of the cell. Compartments of counter (2) and reference (3) electrodes were separated from the main flow of electrolyte by filters (Upchurch Scientific, Oak Harbor, WA, USA). Both electrodes were $Ag/AgCl/1$ M KCl. All reported potentials are given relative to the reference electrode. The analyte stream arrives on the working electrode surface through the outer tube (4) of the two coaxial system and the products of the electrode reaction are transferred to the mass spectrometer through the inner tube (5). The distance between the opening of the coaxial system and the working electrode was 50 μm . All tubes were from PEEK (Upchurch Scientific, Oak Harbor, WA, USA). The inner tube has an inner diameter of 125 μm , an outer diameter of 1.6 mm, and is 15 cm long. The flow of the solution was driven by a syringe pump.

The product stream was diluted with excess methanol. After mixing with methanol, the sample stream was delivered to the ESI interface by tubing that is 30 cm long, and has an inner diameter of 125 μm . The flow rate of the product stream was ca. 35 $\mu\text{L}\cdot\text{min}^{-1}$. The methanol flow in the auxiliary tubing was 30 $\mu\text{L}\cdot\text{min}^{-1}$. The reagent flow rate was set to 5 $\mu\text{L}\cdot\text{min}^{-1}$. The current cell design permitted us to measure mass spectra and linear sweep voltammograms simultaneously.

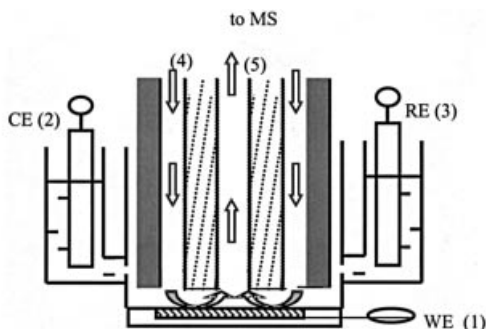


Figure 10. Scheme of the electrochemical cell used in this study: 1: working electrode (WE); 2: counter electrode (CE); 3: reference electrode (RE); 4: outer capillary (transfer line of reagents to working electrode); 5: inner capillary (transfer line of products to the ESI/MS)

Acknowledgments

R. P. thanks the CNRS and the Ministry of Research for funding. A. D. M. and O. L. acknowledge the financial support of the Israel Science Foundation. We are grateful to the French Embassy in Israel for an Arc-en-Ciel/Keshet travel grant and to Prof. M. Vorotyntsev for helpful discussion. We thank a reviewer for very useful comments.

- [1] M. Yamashita, J. B. Fenn, *J. Phys. Chem.* **1984**, *88*, 4451–4459.
- [2] I. I. Stewart, *Spectrochim. Acta, Part B* **1999**, *54*, 1649–1695.
- [3] X. W. Wei, Z. Xu, *Chin. J. Org. Chem.* **1999**, *19*, 97–103.
- [4] J. C. Traeger, *Int. J. Mass Spectr.* **2000**, *200*, 387–401.
- [5] M. L. Vestal, *Mass Spectrom. Rev.* **1983**, *2*, 447–480.
- [6] W. F. Smyth, *Trac-Trends Anal. Chem.* **1999**, *18*, 335–346.
- [7] G. Wolfbauer, A. M. Bond, D. R. MacFarlane, *J. Chem. Soc., Dalton Trans.* **1999**, 4363–4372.

- [8] A. M. Bond, R. Colton, D. G. Humphrey, P. J. Mahon, G. A. Snook, V. Tedesco, J. N. Walter, *Organometallics* **1998**, *17*, 2977–2985.
- [9] X. Xu, W. Lu, R. B. Cole, *Anal. Chem.* **1996**, *68*, 4244–4253.
- [10] W. Lu, X. Xu, R. B. Cole, *Anal. Chem.* **1997**, *69*, 2478–2484.
- [11] F. Zhou, G. J. Van Berkel, *Anal. Chem.* **1995**, *67*, 3643–3649.
- [12] H. Deng, G. J. Van Berkel, *Anal. Chem.* **1999**, *71*, 4284–4293.
- [13] M. C. S. Regino, A. BrajterToth, *Electroanalysis* **1999**, *11*, 374–379.
- [14] J. Gun, A. Modestov, O. Lev, D. Saurenz, M. A. Vorotyntsev, R. Poli, *Eur. J. Inorg. Chem.*, **2003**, 482–492.
- [15] F. Demirhan, P. Richard, R. Poli, *Inorg. Chim. Acta*, in press.
- [16] H. Arzoumanian, A. Baldy, M. Pierrot, M. Pettrignani, *J. Organomet. Chem.* **1985**, *294*, 327–331.
- [17] E. de Jesus, A. Vazquez de Miguel, P. Royo, A. M. M. Lanfredi, A. Tiripicchio, *J. Chem. Soc., Dalton Trans.* **1990**, 2779–2784.
- [18] D. Saurenz, F. Demirhan, P. Richard, R. Poli, H. Sitzmann, *Eur. J. Inorg. Chem.* **2002**, 1415–1424.
- [19] E. J. Alvarez, V. H. Vartanian, J. S. Brodbelt, *Anal. Chem.* **1997**, *69*, 1147–1155.
- [20] M. J. Van Stipdonk, M. P. Ince, B. A. Perera, J. A. Martin, *Rapid Commun. Mass Spectr.* **2002**, *16*, 355–363.
- [21] A. J. Gordon, R. A. Ford, *The Chemist's Companion. Handbook of Practical Data, Techniques and References*, J. Wiley and Sons, New York, **1983**.
- [22] W. C. Byrdwell, W. E. Neff, *Rapid Commun. Mass Spectr.* **2002**, *16*, 300–319.
- [23] A. K. Vrkcic, R. A. J. O'Hair, *Int. J. Mass Spectr.* **2002**, *218*, 131–160.
- [24] E. Collange, J. Garcia, R. Poli, *New J. Chem.* **2002**, *26*, 1249–1256.
- [25] M. Cousins, M. L. H. Green, *J. Chem. Soc. A* **1969**, 16–19.
- [26] A. L. Rheingold, J. R. Harper, *J. Organomet. Chem.* **1991**, *403*, 335–344.
- [27] V. F. DeTuri, K. M. Ervin, *J. Phys. Chem. A* **1999**, *103*, 6911–6920.
- [28] E. R. Talaty, B. A. Perera, A. L. Gallardo, J. M. Barr, M. J. Van Stipdonk, *J. Phys. Chem. A* **2001**, *105*, 8059–8068.
- [29] K. X. Wan, M. L. Gross, T. Shibue, *J. Am. Soc., Mass Spec.* **2000**, *11*, 450–457.
- [30] J. F. Gal, P. C. Maria, E. D. Raczynska, *J. Mass Spectrom.* **2001**, *36*, 699–716.
- [31] L. Fan, M. L. Turner, M. B. Hursthouse, K. M. A. Malik, O. V. Gusev, P. M. Maitlis, *J. Am. Chem. Soc.* **1994**, *116*, 385–386.
- [32] F. Bottomley, J. Chen, K. F. Preston, R. C. Thompson, *J. Am. Chem. Soc.* **1994**, *116*, 7989–7995.
- [33] J. R. Harper, A. L. Rheingold, *J. Am. Chem. Soc.* **1990**, *112*, 4037–4038.
- [34] F. Demirhan, J. Gun, O. Lev, A. Modestov, R. Poli, P. Richard, *J. Chem. Soc., Dalton Trans.* **2002**, 2109–2111.
- [35] A. Modestov, J. Gun, O. Lev, manuscript in preparation.

Received November 16, 2002